# Tension Robust Control Strategy Based on Self-optimizing Algorithm

Jinbao He, Yongyi He, Shuai Guo, Minglun Fang
College of Electromechanical Engineering
Shanghai University
Robert Center & CIMS, No.149, Yanchang Road, Zhabei District, Shanghai, China, 200072
hejinbao79@yahoo.cn

*Abstract*: In tension systems, the main concern is to decouple the tension and velocity in spite of radius variations and other perturbations. To solve this control problem and design the optimal controller, this paper develops a mixed-sensitivity robust $H_\infty$ control based on self-optimizing algorithm. First, the modeling of the tension system is presented with relative theorems. Second, a mixed-sensitivity robust $H_\infty$ control which reduces the coupling between tension and velocity is compared to PID controller. But the $H_\infty$ controller is conservative, the $H_\infty$ controller method with parameter fuzzification is introduced. At low velocity, the $H_\infty$ control method with parameter fuzzification gets fine results. However, for the high velocity and real time requirements of tension system, the $H_\infty$ control method with parameter fuzzification cannot keep the controller optimal always. Therefore the tension robust control strategy based on self-optimizing algorithm is proposed. The controller is optimized by hyper generation GA (HGGA) which reduces computing time. Furthermore, the current error and the change of the error are turned to compensate time delay. In order to test the effectiveness of the proposed algorithms, the tension experiment platform analog system is developed based on DSP (TMS320LF2407A) board. Finally the algorithms in this paper are tested in tension system platform, and the feasibility has been verified.

*Key-Words*: tension system; robust control; parameter fuzzification; genetic algorithm (GA); hyper generation GA (HGGA); time delay; DSP;

## 1 Introduction

Tension control is a kind of common technology and is widely used in the engineering industry such as printing equipment，papermaking, fiber winding. Tension control technology is a great project to be solved for the technician. The main objective of tension control is to increase as much as possible the transport velocity while controlling the tension of the elastic material. Generally, proportional-integral-derivative (PID) is used in industry. However, in high velocity applications, PID becomes unsatisfying.

There are many problems in tension systems that must be solved. Due to the variation of the radius and the inertia of the rollers, the winding process is complex. Furthermore, there is the strong coupling between material velocity and tension. So, tension system is more difficult to control than other systems.

In the last few decades, several methods are available for tension control. The linear parameter varying (LPV) and robust $H_\infty$ control strategy (see [2]) with varying gains are combined to give fine results, for the robustness to radius and inertia changes. In paper [3], multivariable robust control with two degrees of freedom (2DOF) and gain scheduling applied to winding systems is presented. Three controller structures are considered: a global controller, a semi-decentralized controller, and a semi-decentralized controller with overlapping. Two new tension estimators are proposed in [4], and the estimators consider all essential dynamic, friction, inertial variation effects. The robust inferential controller based on quantitative feedback theory is developed for hot strip mill tension control in [5]. Multivariable control strategies have been proposed for industrial metal transport systems [6]-[7].

However, above algorithms are complicated and require large computational time. To accomplish the mentioned motivation, tension robust $H_\infty$ control based on self-optimizing algorithm is developed in this paper. Due to the mixed-sensitivity $H_\infty$ controller's conservatism, the $H_\infty$ control method with parameter fuzzification is studied, which can restrain interference and decrease the coupling degree between velocity and tension. The experiment results demonstrate the tracking performance of robust $H_\infty$ controller with parameter fuzzification at low velocity. Nevertheless, for the high velocity and real time requirements of tension system, the robust $H_\infty$ controller should be improved. So the tension robust control strategy based on self-optimizing algorithm is proposed. The optimizing method for the robust controller based on hyper generation genetic algorithm (HGGA) is presented. Furthermore, the current error and the change of the error are turned to compensate time delay. Finally the algorithms above are tested in tension platform, and the feasibility has been verified.

In the following section of this paper presents the plant modeling of tension system with relative theorems. The third section shows the mixed-sensitivity $H_\infty$ robust control method. Section four gives the tension robust control with parameter fuzzification. The tension robust control strategy based on self-optimizing algorithm is developed in section five. Section six gives experiment results analysis. The experiments are implemented based on DSP (TMS320LF2407A), a 16-bit digital signal processor.

# 2 Plant Modeling

Fig.1 shows the scheme of experimental system with two motors. The system inputs are the control signals $U_{\mathrm{u}}$ and $U_{\mathrm{w}}$, and the outputs are the unwinding web tension $T_{\mathrm{u}}$ and winding web tension $T_{\mathrm{w}}$. In Fig.1, $V_{\mathrm{i}}(\mathrm{i}=1,\cdots 6)$ and $R_{\mathrm{i}}(\mathrm{i}=1,\cdots 6)$ are the velocities and radius of rollers. $T_{\mathrm{uref}}$ and $T_{\mathrm{wref}}$ are the given web tension values.

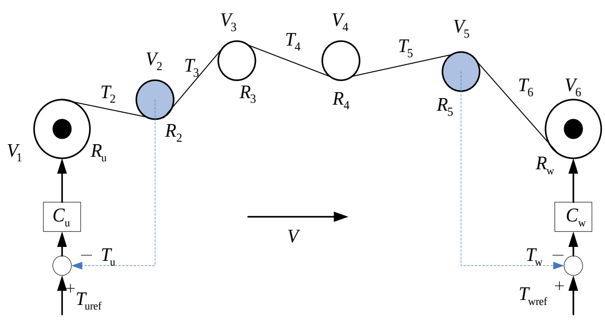


Fig.1 Decentralized tension control system

## 2.1 Web Tension between Two Rolls

The web tension between two rolls can be computed based on three laws [2][3]: Hooke's law, Coulomb's law and Mass conservation law.

● Hooke's law

$$T = EA\varepsilon = EA\frac{L - L_0}{L_0} \tag{1}$$

where $T$ is the tension, $E$ is Young's modulus, $A$ is the web section, $\varepsilon$ is the web strain, $L$ is the web length under stress and $L_0$ is the nominal web length.

● Coulomb's law: The web strain between the first contact point of roll and the first contact point of the following roll is given by

$$\varepsilon(x,t) = \begin{cases} \varepsilon_1(t) & if \quad x \le a \\ \varepsilon_2(t)e^{\mu(x-a)} & if \quad a \le x \le a+g \\ \varepsilon_2(t) & if \quad a+g \le x \le L_{\mathrm{b}} \end{cases} \tag{2}$$

where $a$ is the length of roll sticking zone, $g$ is the length of roll sliding zone, $\mu$ is the friction coefficient and $L_{\mathrm{b}} = a + g + L$.

● Mass conservation law

Suppose an element of web of length $l = l_0(1+\varepsilon)$

$$\rho_0 A L_0 = \rho A L \ \Rightarrow \ \frac{\rho}{\rho_0} = \frac{1}{1+\varepsilon} \tag{3}$$

Where $\rho_0$ and $\rho$ are density between the state without stress and the state under stress.

The web tension equation can be simplified by using Hooke's law, Coulomb's law and Mass conservation law

$$L_{\mathrm{k}-1}\frac{dT_{\mathrm{k}}}{dt} = EA(v_{\mathrm{k}} - v_{\mathrm{k}-1}) + T_{\mathrm{k}-1}v_{\mathrm{k}-1} - T_{\mathrm{k}}(2v_{\mathrm{k}-1} - v_{\mathrm{k}}) \tag{4}$$

where $V_{\mathrm{k}}(\mathrm{k}=1,\cdots,6)$ is the velocity of roll, $T_{\mathrm{k}}(\mathrm{k}=2,\cdots,6)$ is the web tension, and $T_2 = T_{\mathrm{u}}, T_6 = T_{\mathrm{w}}$. A linearized model can be expressed as (e.g. $\mathrm{k}=2$):

$$L_1\frac{dT_2}{dt} = (EA + T_2)(V_2 - V_1) + V_1(T_1 - T_2) \tag{5}$$

where $T_0$ and $V_0$ are the expected values, and $T_2 = T_0$, $V_1 = V_0$.

## 2.2 Velocity Equation of Roll

Assuming the web velocity is equal to the roll linear velocity, the velocity of roll can be got through a torque balance.

Unwinding roll

$$\frac{d(J_{\mathrm{u}}\Omega_{\mathrm{u}})}{dt} = R_{\mathrm{u}}T_2 - K_{\mathrm{u}}U_{\mathrm{u}} - f_{\mathrm{vu}}\Omega_{\mathrm{u}} \qquad (6)$$

Winding roll

$$\frac{d(J_{\mathrm{w}}\Omega_{\mathrm{w}})}{dt} = -R_{\mathrm{w}}T_6 + K_{\mathrm{w}}U_{\mathrm{w}} - f_{\mathrm{vw}}\Omega_{\mathrm{w}} \qquad (7)$$

Dance arm and other rolls

$$J_3\frac{d(v_3)}{dt} = R_3^2(T_4 - T_3) - f_2 v_3 \qquad (8)$$

where $\Omega_{\mathrm{u}}$ and $\Omega_{\mathrm{w}}$ are the rotational speed of unwinding roll and winding roll, $J_{\mathrm{u}}$ and $J_{\mathrm{w}}$ are the roll inertia of unwinding roll and winding roll, $f_{\mathrm{vu}}$, $f_{\mathrm{vw}}$ and $f_2$ are the viscous factor of unwinding roll, winding roll and rolls. $K_{\mathrm{u}}$ and $K_{\mathrm{w}}$ are the constant coefficient of motors.

The state-space representation of nominal model can be written as

$$\begin{cases} \dot{X} = A(t)X + Bu \\ y = CX \end{cases} \qquad (9)$$

where

$X^{\mathrm{T}} = (J_{\mathrm{u}}\Omega_{\mathrm{u}} \quad T_2 \quad V_2 \quad T_3 \quad V_3 \quad T_4 \quad V_4 \quad T_5 \quad V_5 \quad T_6 \quad J_{\mathrm{w}}\Omega_{\mathrm{w}})$

$U^{\mathrm{T}} = (U_{\mathrm{u}} \quad U_{\mathrm{w}})$

$Y^{\mathrm{T}} = (T_{\mathrm{u}} \quad T_{\mathrm{w}}) = ((\alpha T_2 + \beta T_3) \quad (\beta T_5 + \alpha T_6))$

Matrices $A(t), B, C$ are given in the Appendix.

## 3 Tension Mixed-sensitivity Robust $H_\infty$ Control

The mixed-sensitivity robust $H_\infty$ control can reduce the coupling between web tension and velocity, and it is a powerful tool to design tension controller with properties of disturbances rejection.

The transfer function of unwinding roll is obtained using the state-space representation of nominal model and equation (5)

$$G_{\mathrm{u}}(s) = \frac{T_2(s)}{U_{\mathrm{u}}(s)} = \frac{E_1L_1K_{\mathrm{u}}R_{\mathrm{u}}}{J_{\mathrm{u}}L_1s^2 + (f_{\mathrm{u}}J_{\mathrm{u}}L_1 + J_{\mathrm{u}}V_0)s + f_{\mathrm{u}}J_{\mathrm{u}}V_0 + E_1L_1R_{\mathrm{u}}^2} \qquad (10)$$

The transfer function of wingding roll can be rewritten as

$$G_{\mathrm{w}}(s) = \frac{T_6(s)}{U_{\mathrm{w}}(s)} = \frac{E_5L_5K_{\mathrm{w}}R_{\mathrm{w}}}{J_{\mathrm{w}}L_5s^2 + (f_{\mathrm{w}}J_{\mathrm{w}}L_5 + J_{\mathrm{w}}V_0)s + f_{\mathrm{w}}J_{\mathrm{w}}V_0 + E_5L_5R_{\mathrm{w}}^2} \qquad (11)$$

The robust $H_\infty$ controller is designed using the mixed sensitivity approach, as shown in Fig.2. In this figure, $w$ are exogenous signals, $e$ is the error variable, $u$ is the control signals, $y$ is the measured variables, $z$ is the output signals.

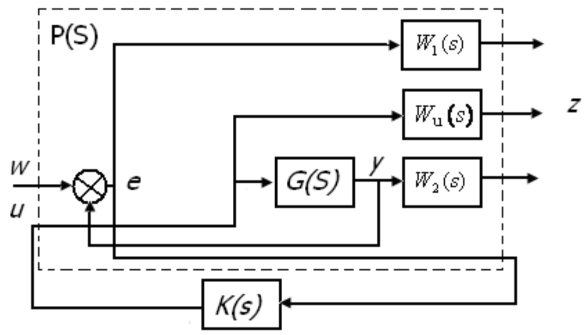


Fig.2 mixed sensitivity robust $H_\infty$ control

It can be seen that generalized plant $P(S)$ is composed of nominal plant $G(S)$ and a set of weighting matrices $W_1(s)$, $W_2(s)$, and $W_u(s)$. The expression of the closed loop transfer function $T_{zw}(s)$ using linear fractional transformation (LFT) is as follows

$$T_{\mathrm{zw}}(s) = \begin{bmatrix} W_1S \\ W_{\mathrm{u}}KS \\ W_2T \end{bmatrix}$$

where $S$ is the sensitivity function, $S = (I + GK)^{-1}$, and $T$ is the complementary sensitivity function, $T = I - S$.

The sensitivity function $S$ represents the perturbation's influence on the measurement outputs. The complementary sensitivity function $T$ represents the influence of the measurement noise on the measurement outputs. $KS$ represents the impact of the perturbation on control signals. To ensure perturbation rejection, the $S$ must be minimized, and to handle noise rejection, the $T$ have to be minimized. This synthesis may seem contradictory. In order to solve this problem, weighting matrices $W_1(s)$, $W_2(s)$, and $W_u(s)$ are introduced in different frequency ranges.

The design objective is to minimize a weighted mix of the transfer function $S$ and $T$ in different frequency ranges. This mixed sensitivity design objective can be formulated as follows: Given

$P(S)$ and $\gamma > 0$, finding controller $K(S)$ which stabilizes the closed loop system and ensures

$$\|T_{zw}\|_\infty = \sup_\omega \sigma_{\max}(T_{zw}(j\omega)) \le \gamma \qquad (12)$$

$\gamma$ is the achieved value of the optimum. Weighting matrices can be adjusted so that $\gamma$ is inferior and close to 1. The synthesis of controller using $S/KS/T$ mixed sensitivity configuration requires the choice of three weighting matrices $W_1(s)$, $W_2(s)$, and $W_u(s)$. These matrices are supposed to be chosen following procedure.

$W_1(s)$ and $W_2(s)$ are weight matrices for shaping the characteristics of open-loop plant. The standard practice is to choose the weighting matrix $W_1(s)$ with high gain at high at low frequencies in order to reject low-frequency output disturbances. The weighting matrix $W_2(s)$ should be a high-pass filter in order to ensure robustness against additive uncertainties in the plant model in the high-frequency range. The weighting matrix $W_u(s)$ is used to avoid large control signals. The following conditions are necessary and sufficient for robust stability, nominal and robust performance.

$$\|W_1 S\| < 1,\ \|W_2 T\| < 1 \quad \Rightarrow$$

$$\bar{\sigma}(S(j\omega)) \le \left|W_1^{-1}(j\omega)\right|,\ \bar{\sigma}(T(j\omega)) \le \left|W_2^{-1}(j\omega)\right|$$

# 4 Tension Mixed-sensitivity Robust $H_\infty$ Controller with Parameter Fuzzification

## 4.1 Robust Controller with Parameter Fuzzification Design

The mixed-sensitivity robust $H_\infty$ control improves robustness to the change of radius and inertia of tension systems, but robust $H_\infty$ control is based on a worst-case design and could be overly conservative for a large parameter set. While fuzzy method develops relying on expert experiences and it is easy to realize. The $H_\infty$ controller with parameter fuzzification is designed to control tension in this part.

The tension controller is chosen according to the error and the change of error. As aforementioned in section three, $\|S\|_\infty$ is the measurement of tracking capability and disturbance suppression. When $\|S\|_\infty$ decreases, the robust controller plays an increasing dominant regulation role and enhances the speed. So, the $H_\infty$ controller can be defined as following, the standard controller means the most conservative $H_\infty$ controller, the enhanced controller means the $H_\infty$ controller with the min-nom.

Suppose that the tension robust controller $K_0(s)$ is the standard controller, $K_2(s)$ is the enhanced controller, and $K_1(s)$ is the controller that its control ability is between the standard controller and enhanced controller. Each of the input variables has following sets: NB, NS, ZO, PS, PB. Rules are constructed in a 5*5 fuzzy table as shown in table 1.

Tabel1 the rules of tension robust controller

| $E_c$ \ $E$ | NB | NS | ZO | PS | PB |
|---|---|---|---|---|---|
| NB | $K_2(s)$ | $K_2(s)$ | $K_1(s)$ | $K_1(s)$ | $K_1(s)$ |
| NS | $K_2(s)$ | $K_1(s)$ | $K_1(s)$ | $K_0(s)$ | $K_1(s)$ |
| ZO | $K_1(s)$ | $K_1(s)$ | $K_0(s)$ | $K_1(s)$ | $K_1(s)$ |
| PS | $K_1(s)$ | $K_0(s)$ | $K_1(s)$ | $K_1(s)$ | $K_2(s)$ |
| PB | $K_1(s)$ | $K_1(s)$ | $K_1(s)$ | $K_2(s)$ | $K_2(s)$ |

## 4.2 Experimental Results

The proposed robust $H_\infty$ control with parameters for tension system has been implemented on a laboratory drive. The drive is shown in Fig.3. The DSP-based control card (TMS320 LF2407A) is installed in the control computer which has multi channels of D/A, A/D, I/O and encoder interface circuits. Contrast table of amplitude and tension is shown in Table 2.

Fig.3 experimental setup

Table 2 contrast table of amplitude and tension

| Amplitude | Tension(kg) |
|---|---|
| 2500 | 0.512 |
| 2600 | 0.471 |
| 2700 | 0.430 |
| 2800 | 0.389 |
| 2900 | 0.348 |
| 3000 | 0.307 |
| 3100 | 0.266 |
| 3200 | 0.225 |

The control using PID controllers and the $H_\infty$ robust control are compared on Fig.4 under speed $1000 r/\min$. The square reference tension is periodic that change between 2700 and 3000 about 2 seconds. From the experimental results, it is hard to solve the tension overshoot and stable error using PID controllers. The $H_\infty$ robust control has improved the tracking properties and suppressed the coupling. However, the error at stable stage isn't ideal, the $H_\infty$ robust control with fuzzification is studied.

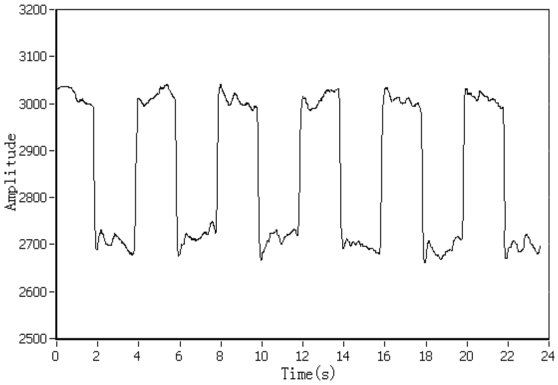


(4a) unwinding web tension using PID

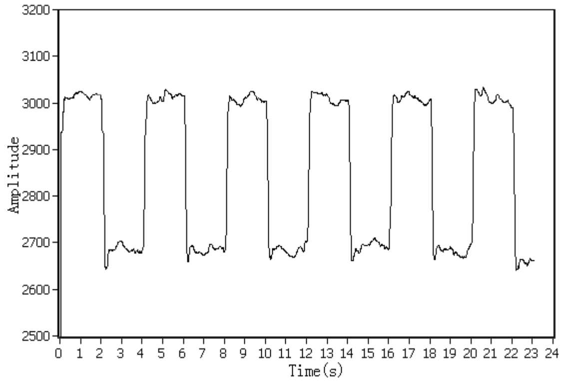


(4b) unwinding web tension using $H_\infty$ control

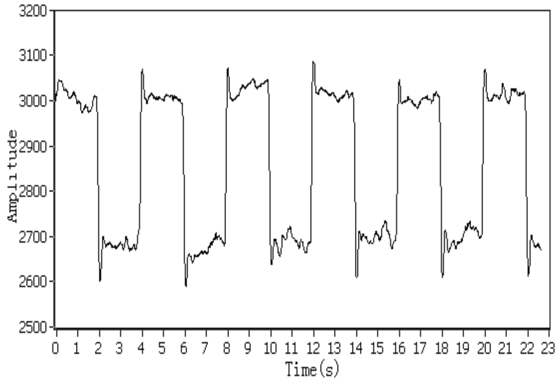


(4c) winding web tension using PID

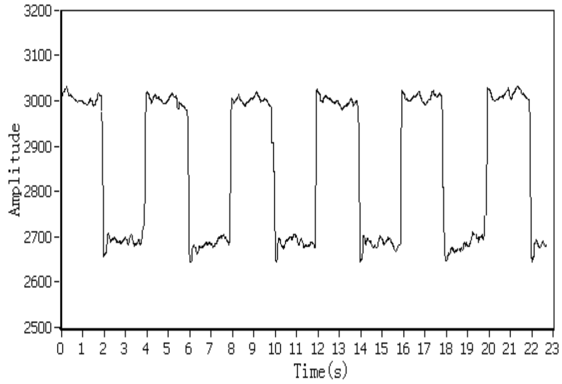


(4d) winding web tension using $H_\infty$ control

Fig.4 PID and $H_\infty$ control

In terms of the model of tension system, the controller can be designed as

$$K(s) = \frac{k(s+a)(s+b)}{(s+c)(s+d)(s+e)} \tag{13}$$

Under $V_0 = 2400r/\min$ , $T_0 = 4.5N$ , the weighting matrices of $G_w(s)$ can be chosen as

$$W_1(s) = \frac{0.5s+10}{s+0.01}, \quad W_u(s) = 0.01$$

$W_2(s)$ is chosen as $s$, $0.01s$ and $0.1s$ which correspond to $K_0(s)$, $K_2(s)$, and $K_1(s)$.

The curves 1, 2 and 3 correspond to the bode of $K_0(s)$, $K_1(s)$ and $K_2(s)$ separately in Fig.5, which satisfying $\|T_{zw}\|_\infty \le 1$.

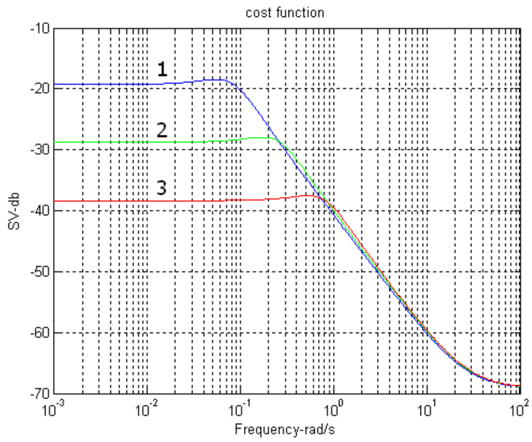


Fig.5 Bode of closed loop $T_{zw}$

In Fig.6 and Fig.7, the bode of $S(s)$ and $T(s)$ (curve 1, 2 and 3) correspond to three cases in Fig.5. The curves 4 are $W_1^{-1}$ (Fig.6) and $W_2^{-1}$ (Fig.7), which satisfying $\bar{\sigma}(S(j\omega)) \le |W_1^{-1}(j\omega)|$ , $\bar{\sigma}(T(j\omega)) \le |W_2^{-1}(j\omega)|$

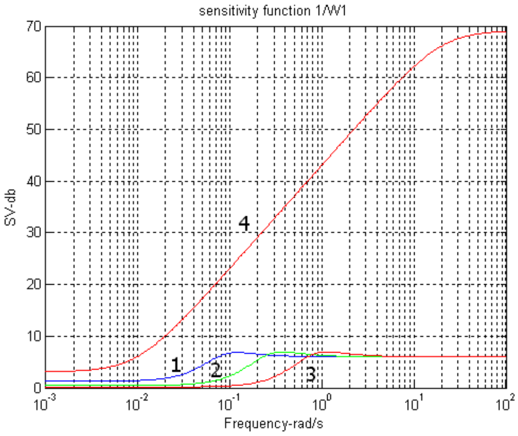


Fig.6 Bode of $S(s)$ and $W_1^{-1}$

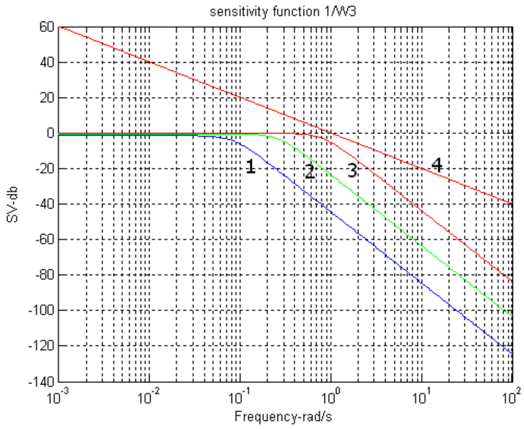


Fig.7 Bode of $T(s)$ and $W_2^{-1}$

Fig.8 shows the experiment results using $H_\infty$ controller with parameter fuzzification at a rotor speed approximately $1000r/\min$ and $2400r/\min$. At low speed $1000r/\min$, the $H_\infty$ control method with parameter fuzzification gets fine results. However, at high speed $2400r/\min$, the tension fluctuation is hard to meet the high precise demands of tension system. The results indicate that the $H_\infty$ control method with parameter fuzzification cannot keep the controller optimal during the whole process. So the tension robust control strategy based on self-optimizing algorithm is proposed, which is introduced in the following paragraph.

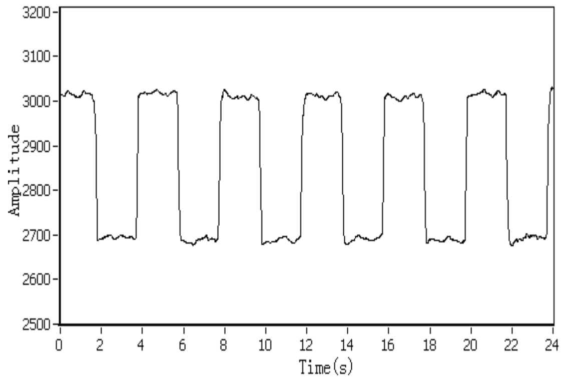


(8a) unwinding web tension ($1000r/\min$)

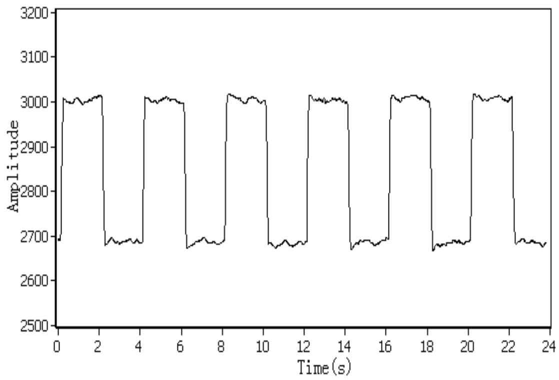


(8b) winding web tension ($1000r/\min$)

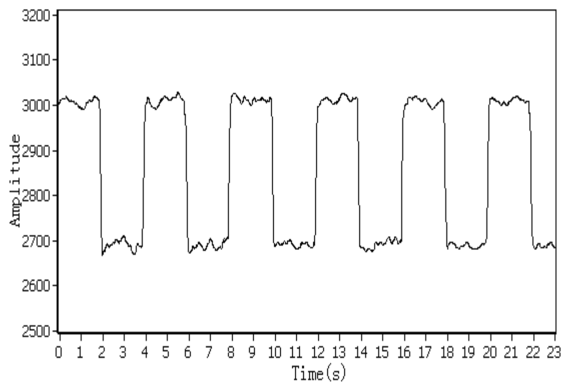


(8c) unwinding web tension ($2400r/\min$)

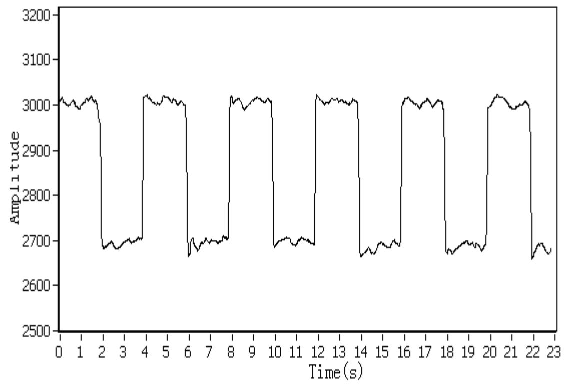


(8d) winding web tension ($2400r/\min$)

Fig. 8 $H_\infty$ control with parameter fuzzification

## 5 Tension Robust Control Strategy Based on Self-optimizing Algorithm

As aforementioned, the robust control strategy based on self-optimizing algorithm is proposed to meet the high precise demands of tension system in this part. The self-optimizing algorithm is used to obtain optimal controller between standard controller and enhanced controller during the process. While, in tension systems, there are real-time problems that require a short response time and fast convergence speed. To address this, this paper adopts hyper generation genetic algorithm (HGGA) [14] to obtain optimal controller.

The characteristic of conventional genetic algorithm (GA) slowly converges to an optimal solution, which limits its application in real time system. The methods to improve the convergence speed of Genetic Algorithms (GAs) have received significant interest. A genetic algorithm (GA) using linear approximation of load flow equation and heuristic selection of participating controls were combined in a search method for the minim number of control actions [15]. An on-line genetic approach optimizes the input/output membership functions and gains [16]. In [17], using symbiotic evolution based fuzzy controller design method, the number of control trials and consumed CPU time are considerably reduced when compared to traditional GA-based fuzzy controller design methods. However, these methods is hard to realized and the evolution speed is still limited. This paper proposes HGGA to improve the convergence speed of GA for tension systems.

## 5.1 Self-optimizing Algorithm on Line

In this section, the $H_\infty$ controller is optimized on line by hyper generation GA (HGGA) which reduces computing time. Furthermore, the current error and the change of the error are turned to compensate time delay.

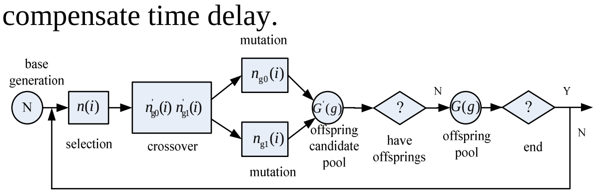


Fig.9 Block diagram of HGGA

**HGGA(hyper generation GA)**: The conventional GA is generation-based scheme, which processes chromosomes generation by generation. The evolutionary process including crossover, mutation and selection performs in the same generation. The selection operation is only triggered until N offspring candidates are generated, which takes long time to wait and limits the evolution speed. To overcome the drawbacks of conventional GA, the HGGA is introduced.

As shown in Fig.9, the GA operations, crossover, mutation, and selection in HGGA are the same as those in conventional GA. The key feature of HGGA is to break the generation restrain to accelerate convergence speed. Namely, the GA operations are not limited in the same generation. When an offspring is generated, the HGGA allows the offspring to mate with one of the unprocessed chromosomes immediately. The new offspring chromosomes may be generated from parent mating with offspring. The offspring is no longer consumed long waiting time. Additionally, the offspring stored in candidate pool enter the offspring pool only when there is no chromosome in offspring pool. Then, the GA operations, selection, crossover, and mutation, are triggered immediately.

**Dynamic Fitness Function:** The fitness function is used to evaluate chromosomes during selection operation to determine which offspring should be remained as the parents for next generation. Due to time delay, $e(t)$ is the error of $t-kT$ in fact, while the current control effect will be indicated in time point $t+kT$ . This paper presents a dynamic fitness function to compensate time delay. In fitness function, the error $e(t+kT)$ and change of error $\dot{e}(t+kT)$ in time point $t+kT$ are predicted in terms of current error $e(t)$ . The dynamic fitness function can be expressed as

$$FIT_2 = \exp[-(\alpha^2 z_1^2 + z_2^2 / \alpha^2)] \qquad (14)$$

Where $z_1 = e$ , $z_2 = \dot{e}$, $\alpha$ is a constant and can be chosen according to actual system. In this paper,

(1) if $|z_2| < \delta$ , then $\alpha = 1$ ;

(2) if $|z_2| > \delta$ , $|z_1(KT)| < |z_1(KT+T)|$ , then $\alpha = 1.1$ ;

(3) if $|z_2| > \delta$ , $|z_1(KT)| \geq |z_1(KT+T)|$ , then $\alpha = 0.9$ .

where $\delta$ is a constant and $\delta = 0.2$ in this paper.

## 5.2 Experimental Results

The robust controller based on self-optimizing is searched in the range from the enhanced controller to standard controller in section four. In terms of the error and change of error, the range can be divided into two groups. Namely, one group is between the standard controller $K_0(s)$ and $K_1(s)$ , the other group is between $K_1(s)$ and enhanced controller $K_2(s)$ . Thus narrowing the range, the robust controller can be obtained exactly. From section four, there are 6 parameters in each controller. For each population member, a binary string length of 96 bits is used.

When the error increases and $FIT_2 < \varepsilon$ ($\varepsilon > 0$), the HGGA starts to execute selection operation. Initially, 8 chromosomes in the base generation have been generated. First, the fitness value of each chromosome is calculated. Then, the new offspring is generated by HGGA and the fitness value can be obtained. The optimal scheduling result will be the chromosome with the larger fitness value. Finally, the 8 optimal chromosomes will be regarded as base generation for next HGGA. Because of the specialty of tension system, the HGGA follows these principles:

(1) Deal with offspring firstly; (2) Allow the chromosome to mate with chromosome in different generation firstly; (3) Two parent chromosomes generate two offspring chromosomes, and two chromosomes with the largest fitness value are remained.

Fig.10 shows the experiment results using robust $H_\infty$ controller based on self-optimizing at a rotor speed approximately $2400 r/\min$. For the exerting disturbance case, as shown in Fig.10c and Fig.10d, the error at stable stage is ideal. Therefore, in the case of high speed and disturbance, the robust controller based on self-optimizing shows superior performance.

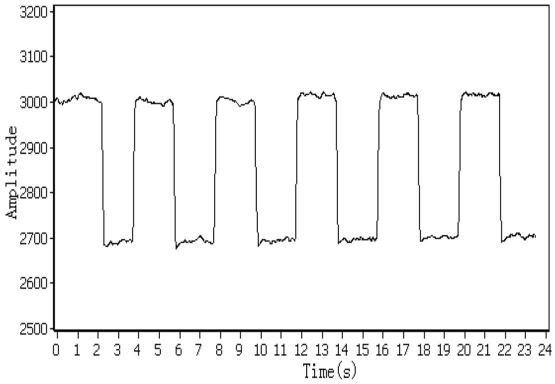

(10a) unwinding web tension

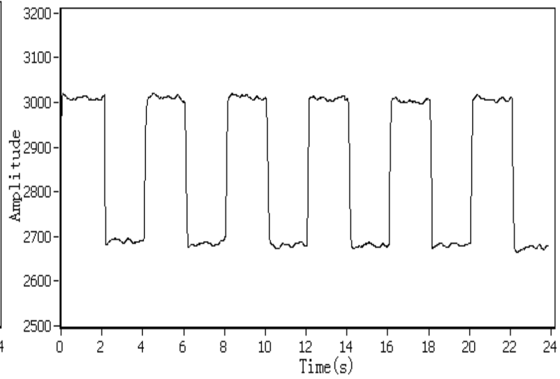

(10b) winding web tension

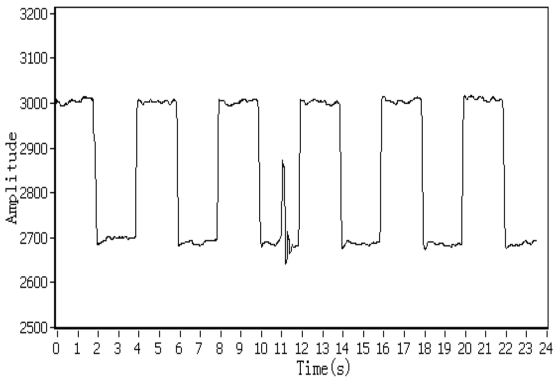

(10c) unwinding web tension under disturbance

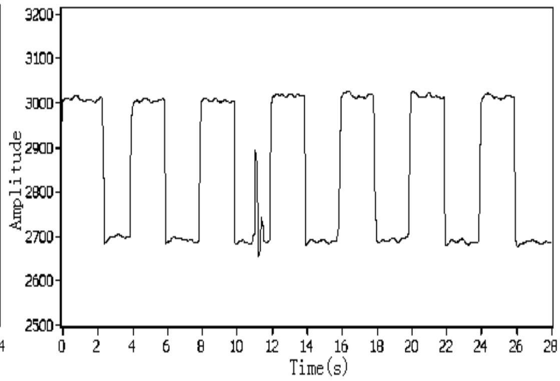

(10d) winding web tension under disturbance

Fig.10 Robust controller based on self-optimizing ( $2400\ r/\min$ )

## 6 Experiment Results Analysis

In order to explain the performance of proposed controllers, we analyze the tension static difference ratio and tension fluctuation ratio. The static difference ratio is an important evaluation index of tension systems, and the fluctuation ratio is the key index of tension systems.

The static difference ratio $\delta$ of tension is defined as

$$\delta = \frac{2(T_{\max} - T_{\min})}{(T_{\max} + T_{\min})} \times 100\% \qquad (15)$$

where $T_{\max}$ represents the max value of tension, $T_{\min}$ represents the min value of tension.

The fluctuation ratio $\xi$ of tension is defined as

$$\xi = \frac{T_{\max} - T_{\min}}{T_r} \times 100\% \tag{16}$$

where $T_r$ represents the given value of tension.

From Fig.4a, Fig.4c, Fig.8a and Fig.8b, the static difference ratio $\delta_i, \delta_i^*(i = 1, 2, 3, 4)$ and fluctuation ratio $\xi_i, \xi_i^*(i = 1, 2, 3, 4)$ can be calculated.

1.In the case of given amplitude 2700, $\omega = 1000r/\min$ and unwinding, $H_\infty$ robust controller with parameter fuzzification: $\delta_1 = 2.8\%$, $\xi_1 = 2.9\%$ ;PID controller: $\delta_1^* = 5.4\%$, $\xi_1^* = 5.5\%$

2.In the case of given amplitude 3000, $\omega = 1000r/\min$ , and unwinding, $H_\infty$ robust controller with parameter fuzzification: $\delta_2 = 2.9\%$, $\xi_2 = 2.8\%$; PID controller: $\delta_2^* = 6.2\%$, $\xi_2^* = 6.3\%$

3.In the case of given amplitude 2700, $\omega = 1000r/\min$ , and winding, $H_\infty$ robust controller with parameter fuzzification: $\delta_3 = 2.8\%$, $\xi_3 = 2.9\%$; PID controller: $\delta_3^* = 5.8\%$, $\xi_3^* = 5.9\%$

4.In the case of given amplitude 3000, $\omega = 1000r/\min$ , and winding, $H_\infty$ robust controller with parameter fuzzification: $\delta_4 = 3.0\%$, $\xi_4 = 2.9\%$; PID controller: $\delta_4^* = 6.1\%$, $\xi_4^* = 6.3\%$

From Fig.8c, Fig.8d, Fig.10a and Fig.10b, the static difference ratio $\delta_i, \delta_i^*(i = 5, 6, 7, 8)$ and fluctuation ratio $\xi_i, \xi_i^*(i = 5, 6, 7, 8)$ can be calculated.

5.In the case of given amplitude 2700, $\omega = 2400r/\min$, and unwinding, robust controller based on self-optimizing: $\delta_5 = 2.7\%$, $\xi_5 = 2.8\%$; $H_\infty$ robust controller with parameter fuzzification: $\delta_5^* = 4.4\%$, $\xi_5^* = 4.5\%$

6.In the case of given amplitude 3000, $\omega = 2400r/\min$, and unwinding, robust controller based on self-optimizing: $\delta_6 = 2.8\%$, $\xi_6 = 2.8\%$; $H_\infty$ robust controller with parameter fuzzification: $\delta_6^* = 4.5\%$, $\xi_6^* = 4.4\%$

7.In the case of given amplitude 2700 , $\omega = 2400r/\min$ , and winding, robust controller based on self-optimizing: $\delta_7 = 2.9\%$, $\xi_7 = 3.0\%$; $H_\infty$ robust controller with parameter fuzzification: $\delta_7^* = 4.5\%$, $\xi_7^* = 4.4\%$

8.In the case of given amplitude 3000 , $\omega = 2400r/\min$ , and winding, robust controller based on self-optimizing: $\delta_8 = 3.0\%$, $\xi_8 = 2.9\%$; $H_\infty$ robust controller with parameter fuzzification: $\delta_8^* = 4.3\%$, $\xi_8^* = 4.3\%$

## 7 Conclusion

The radius and the inertia of tension systems vary on a large scale, changing considerably the system dynamics. The $H_\infty$ robust controller has shown good performance in robustness to radius variation and decoupling between speed and tension compared to classical PID controller.

To further improve stability and performance a $H_\infty$ robust controller with parameters fuzzificaton was proposed, which was shown to effectively control tension with only static difference ratio $3.0\%$ and fluctuation ratio $2.9\%$ at the speed $1000r/\min$. While at high speed $2400r/\min$, the tension fluctuation is hard to meet the high precise demands of tension systems. So the tension robust control strategy based on self-optimizing algorithm is proposed. The $H_\infty$ controller is optimized on line by hyper generation GA (HGGA) which reduces computing time. At high speed $2400r/\min$, static difference ratio $3.0\%$ and fluctuation ratio $2.9\%$ can be obtained by the $H_\infty$ controller based on self-optimizing.

*References:*

[1] Ming D W, Chuen Tsai S. Comments on constraining the optimization of a fuzzy logic controller, *IEEE transaction on systems, man, and cybernetics.*, Vol.31, No.4, 2001, pp.663-666

[2] Hakan Koc, Dominique Knittel, Michel de Mathelin. Modeling and robust control of winding systems for elastic webs, *IEEE Transactions on Control Systems Technology*, Vol.10, No.2, 2002, pp. 197-208

[3] Dominique Knittel, Edouard Laroche, Daniel Gigan. Tension control for winding systems with two-degrees-of-freedom $H_\infty$ controllers , *IEEE Transaction on Industry Applications*, Vol.39, No.1, 2003, pp. 113-120

[4] Carrasco R., Valenzuela. Tension control of a two-drum winder using paper tension

estimation, *IEEE Transaction on Industry Applications*，Vol.42, No.2, 2006, pp. 618-628

[5] G.Hearns, M.J.Grimble. Inferential control for rolling mills, *IEE Proc.-Control Theory Appl.*, Vol.147, No.6, November, 2000

[6] M.J.Grimble, G.Hearns. Advanced control for hot rolling mills. *In Advances in Control, Highlights of ECC'99.* Berlin, Germany: Springer, 1999, pp.135-169

[7] E.J.M.Geddes, I.Postlethwaite. Improvements in product quality in tandem cold rolling using robust multivariable control, *IEEE Trans. Contr: Syst*.,Vol.6, 1998, pp.257-269

[8] Ortega M.G.，Vargas M.，Castano F.，et al. Improved design of the weighting matrices for the S/KS/T mixed sensitivity problem-application to a multivariable thermodynamic system, *IEEE Transactions on Control Systems*，Vol.14, No.1, 2006, pp. 82-90

[9] Luo F.L. Multiple-page-mapping back propagation neural network for constant tension control, *IEE Proceedings Electric Power Applications*，Vol.145, No.3, 1998, pp. 239-245

[10] Seung.-Ho Song，Seung-Ki Su. Design and control of multi-span tension simulator, *IEEE Transactions on Industry Application*，Vol.36, No.2, 2000, pp. 640-648

[11] Zames G. On the input-output stability of time varying nonlinear feedback systems: Parts I and II , *IEEE Tran AC*，Vol.11, No.2-3, 1996, pp. 228-238

[12] He Jinbao，He Yongyi，Guo Shuai. Research of tension robust control based on mixed sensitivity, *ITIC 2006，China*， 2006, pp. 2061-2064

[13] Hinamoto T.，Zempo Y.，Nishino Y.，ET AL. An analytical approach for the synthesis of two-dimensional state-space filter structures with minimum weighted sensitivity, *IEEE Transaction on Circuits and Systems I: Fundamental Theory and Applications* ， Vol.46, No.10, 1999, pp. 1172-1183

[14] Shiann_T S, Yue-R C. A pipeline- based genetic algorithm accelerator for time critical processes in real time systems, *IEEE transactions on computers*， Vol.55, No.11, 2006, pp. 1435-1448

[15] Yair M, Sigmond S. A genetic algorithm for the corrective control of voltage and reactive power, *IEEE Transactions on power systems*，Vol.21, No.1, 2006, pp. 295-300

[16] F.Cupertino, V.Giordano, D.naso, et.al. On-line genetic design of fuzzy controllers for DCdrives with variable load, *Electronics Letters*, Vol.39, No.5, 2003, pp.479-480

[17] Chia F.J., Jiann Y.L., and Chin T.L. Genetic reinforcement learning through symbiotic evolution for fuzzy controller design, I*EEE Transactionson Systems, Man, and Cybernetics*, Vol.30, No.2, 2000,pp.290-302

[18] Yun Y， Gen M. Performance analysis of adaptive genetic algorithm with fuzzy logic and heuristics, *Fuzzy Optimization and Decision Making*， Vol.2, No.2, 2003, pp. 161-175

[19] Liu H B，Xu Z G，Abraham A. Hybrid fuzzy-genetic algorithm approach for crew grouping , *Proc of the 5th Int Cof on Intelligent Systems Design and Applications*，Wroclaw，2005, pp.332-337

[20] Meng Joo Er，Ya Lei Sun. Hybrid fuzzy proportional-integral plus conventional derivative control of linear and nonlinear systems, *IEEE Transactions on Industrial Electronics*， Vol.48, No.6, 2001, pp.1109-1117

[21] Lo K.L，Khan K.. Hierarchical micro-genetic algorithm paradigm for automatic optimal weight selection in H/sub /spl infin// loop-shaping robust flexible AC transmission system damping control design, *IEE Proceedings Generation Transmission and Distribution*， Vol.151, No.1, 2004, pp.109-118

[22] Chunxiang W，Yongzhang W，Ruqing Y，et al. Research on precision tension control system based on network, *IEEE Transaction on Industrial Electronics*，Vol.51, No.2, 2004, pp. 381-386

[23] Shahnazi R.，Akbarzadeh-T M.-R. PI Adaptive Fuzzy Control With Large and Fast Disturbance Rejection for a Class of Uncertain Nonlinear Systems ， *IEEE Transactions on Fuzzy Systems*， Vol. 16, No. 1, 2008, pp.187 – 197

[24] Perales-Gravan C.，Lahoz-Beltra R..An AM Radio Receiver Designed With a Genetic Algorithm Based on a Bacterial Conjugation Genetic Operator, *IEEE Transactions on Evolutionary Computation,* Vol.12, No.2，2008, pp.129 - 142

## Appendix

$$A(t)=$$

$$\begin{bmatrix}
-\frac{f_{\mathrm{vu}}}{J_{\mathrm{u}}(t)} & R_{\mathrm{u}}(t) & 0 & 0 & 0 & 0 & 0 & 0 & 0 & 0 & 0 \\
E_1\frac{R_{\mathrm{u}}(t)}{J_{\mathrm{u}}(t)} & -\frac{V_0}{L_1} & E_1 & 0 & 0 & 0 & 0 & 0 & 0 & 0 & 0 \\
0 & -\frac{R_2^2}{J_2} & -\frac{f_2}{J_2} & \frac{R_2^2}{J_2} & 0 & 0 & 0 & 0 & 0 & 0 & 0 \\
0 & \frac{V_0}{L_2} & -E_2 & -\frac{V_0}{L_2} & E_2 & 0 & 0 & 0 & 0 & 0 & 0 \\
0 & 0 & 0 & -\frac{R_3^2}{J_3} & -\frac{f_3}{J_3} & \frac{R_3^2}{J_3} & 0 & 0 & 0 & 0 & 0 \\
0 & 0 & 0 & \frac{V_0}{L_3} & -E_3 & -\frac{V_0}{L_3} & E_3 & 0 & 0 & 0 & 0 \\
0 & 0 & 0 & 0 & 0 & -\frac{R_4^2}{J_4} & -\frac{f_4}{J_4} & \frac{R_4^2}{J_4} & 0 & 0 & 0 \\
0 & 0 & 0 & 0 & 0 & \frac{V_0}{L_4} & -E_4 & -\frac{V_0}{L_4} & E_4 & 0 & 0 \\
0 & 0 & 0 & 0 & 0 & 0 & 0 & -\frac{R_5^2}{J_5} & -\frac{f_5}{J_5} & \frac{R_5^2}{J_5} & 0 \\
0 & 0 & 0 & 0 & 0 & 0 & 0 & \frac{V_0}{L_5} & -E_5 & -\frac{V_0}{L_5} & E_5\frac{R_{\mathrm{w}}(t)}{J_{\mathrm{w}}(t)} \\
0 & 0 & 0 & 0 & 0 & 0 & 0 & 0 & 0 & -R_{\mathrm{w}}(t) & -\frac{f_{\mathrm{vw}}}{J_{\mathrm{w}}(t)}
\end{bmatrix}$$

$$B=\begin{bmatrix} -K_{\mathrm{u}} & 0 & 0 \\ 0 & 0 & 0 \\ \vdots & \vdots & \vdots \\ 0 & 0 & 0 \\ 0 & 0 & K_{\mathrm{w}} \end{bmatrix}_{11\times 3}, \quad C=\begin{bmatrix} 0 & \alpha & 0 & \beta & 0 & 0 & 0 & 0 & 0 & 0 & 0 \\ 0 & 0 & 0 & 0 & 0 & 0 & 0 & \beta & 0 & \alpha & 0 \end{bmatrix}$$

where $L_{\mathrm{i}}(\mathrm{i}=1,\cdots,5)$ is the length of two roll, $E_1=(EA+T_0)/L_1$, $E_2=(EA+T_0)/L_2$, $E_3=(EA+T_0)/L_3$, $E_4=(EA+T_0)/L_4$, $E_5=(EA+T_0)/L_5$, $\alpha,\beta$ are constant, $0<\alpha,\beta<1$